ACKNOWLEDGMENTS

REFERENCES

1. J. Mitola and G.Q. Maguire, Cognitive radio: Making software radios more personal, IEEE Personal Commun 6 (1999), 13–18.
2. Y. Hur, J. Park, W. Woo, K. Lim, C.-H., Lee, H. S. Kim, and J. Laskar, A wideband analogue multi-resolution spectrum sensing (MRSS) technique for cognitive radio (CR) systems, in Proc.-IEEE International Symp Circuits Syst (2006), 4090–4093.

A HALF MODE SUBSTRATE INTEGRATED EPSILON NEAR ZERO RESONATOR AND NOTCH FILTER

Tejinder Kaur Kataria, Alonso Corona-Chavez, and D. V. B. Murthy
National Institute for Astrophysics, Optics, and Electronics (INAOE), Luis Enrique Erro No. 1, Puebla, 72000 Mexico; Corresponding author: tejinder@ieee.org

ABSTRACT: *In this article a miniaturized, half-mode substrate integrated epsilon near zero (ENZ) tunnel is presented. This structure supports a reflection-less transmission at a single frequency when epsilon is near zero. Moreover, this tunnel is connected to a CRLH filter in a decoupling mode to reject unwanted frequencies. Design methodology, simulation, and measurement results of this structure are presented. © 2010 Wiley Periodicals, Inc. Microwave Opt Technol Lett 52: 1707–1709, 2010; Published online in Wiley InterScience (www.interscience.wiley.com). DOI 10.1002/mop.25297*

1. INTRODUCTION

A new way of engineering devices have emerged with the arrival of metamaterials, because of the capacity of realizing structures with chosen ε and μ values. Epsilon near zero (ENZ) metamaterials is a new approach that allows the wave to propagate with little disturbance to abrupt discontinuities [1]. To achieve ENZ behavior, waveguide technology can be adopted. A rectangular waveguide filled with a dielectric of relative permittivity ε_r operated at the fundamental TE_{10} mode has an effective permittivity, which is inherently frequency dispersive as shown in Eq. (1) [2].

$$\frac{\varepsilon_{\text{eff}}}{\varepsilon_0 \varepsilon_r} = n^2 - \frac{c^2}{4 \varepsilon_r f^2 W_t^2}, \tag{1}$$

where n is the refractive index of the filling material, ε_r is the relative permittivity of the material, c is the speed of light in vacuum, W_t is the waveguide H-plane width, and f is the operation frequency. The effective permeability (μ_{eff}) remains constant with a value of μ_0. This equation shows that below the cutoff frequency the effective permittivity is negative ($\varepsilon_{\text{eff}} < 0$), above cutoff, it is positive ($\varepsilon_{\text{eff}} > 1$); thus at cutoff, $\varepsilon_{\text{eff}} \sim 0$. From here, it is seen that at cutoff the propagation constant is zero ($\beta = 0$), which leads to an infinite phase velocity [3]. As a consequence, a perfectly matched propagation exists, which has been previously reported for antenna matching circuits [4] and for perfectly matched waveguide-bends [5]. Alu and Engheta [6] extended this concept to resonant-like ENZ waveguide tunnels in which the tunneling frequency is completely independent of the length of the tunnel; hence, its size can be miniaturized.

In this article, miniaturized ENZ structures are presented using substrate integrated technology with microstrip excitation. Section II describes the ENZ tunnel at a center frequency (f_0) of 1.85 GHz, where further miniaturization is achieved by using the concept of half mode (HM) waveguide [7]. As an application example, Section III demonstrates the usage of this HM tunnel as a notch filter when cascaded in a decoupling mode to a CRLH filter. Each section presents complete design procedure along with simulation and experimental results.

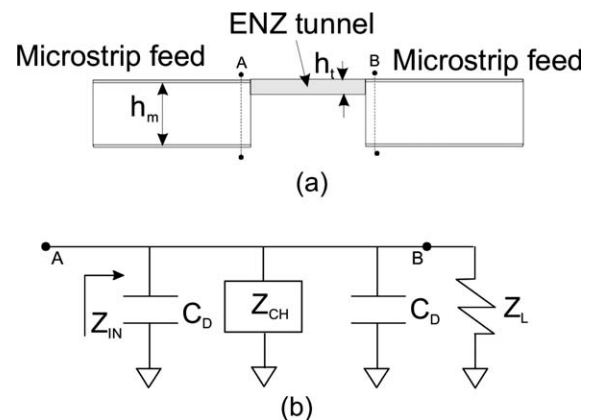## 2. SUBSTRATE INTEGRATED ENZ TUNNELING CIRCUIT

An ENZ tunneling waveguide has a width W_t and height h_t. For the TE_{10} mode, the width of the tunnel can be obtained from Eq. (2).
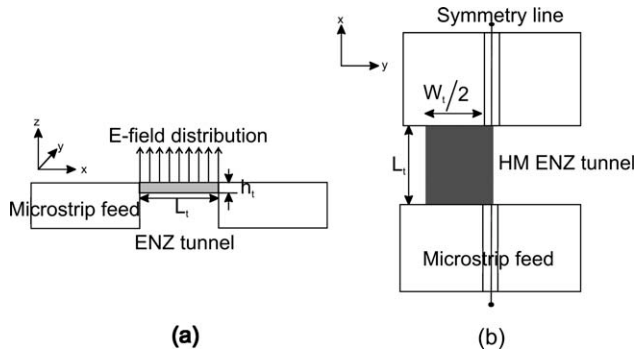
$$W_t = \frac{c}{2 f_0 \sqrt{\varepsilon_r}}, \tag{2}$$

where f_o is the tunneling frequency, c is the speed of light, and ε_r is the relative permittivity. For the selected substrate RT Duroid 5880 ($\varepsilon_r = 2.2$ and height $h_m = 3.2$ mm) and a frequency of operation (f_o) of 1.85 GHz the tunnel width is $W_t = 48$ mm. For the feed line, a 50 Ω microstrip is designed with $W_m = 10$ mm. To tunnel a single frequency, a very abrupt discontinuity between the feed line and the tunnel must exist. This discontinuity can be achieved if the tunnel height is much smaller than the microstrip substrate height ($h_m \gg h_t$) as shown in Figure 1(a). In our case, the tunnel height is fixed to $h_t = 0.5$ mm. Abrupt height changes derive in capacitive-dominant discontinuities, hence the equivalent circuit of Figure 1(b) can be used, where Z_L is the load impedance, C_D is the capacitive discontinuity and Z_{CH} is the characteristic impedance of the waveguide tunnel.

The input impedance Z_{IN} seen at terminal A of the tunnel can be calculated from

$$Z_{IN} = Z_{eq} \frac{Z_L + j Z_{eq} Tan(\beta L_t)}{Z_{eq} + j Z_L Tan(\beta L_t)}, \tag{3}$$

Figure 1 (a) Side view of microstrip-fed ENZ tunnel with large discontinuity and (b) equivalent circuit

Figure 2 (a) E-field distribution of ENZ tunneling structure along propagation direction x, (b) HM ENZ tunneling structure
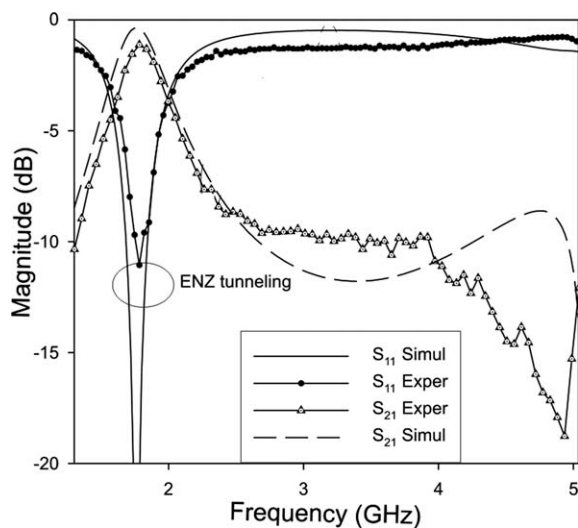
where $Z_{eq} = Z_D \| Z_{CH} \| Z_D$, Z_D is the impedance associated to C_D, L_t is the length of the tunnel, and β is the phase constant.

From here, it can be seen that a perfectly matched condition exists when $\beta = 0$, which occurs when $\varepsilon_{eff} = 0$.
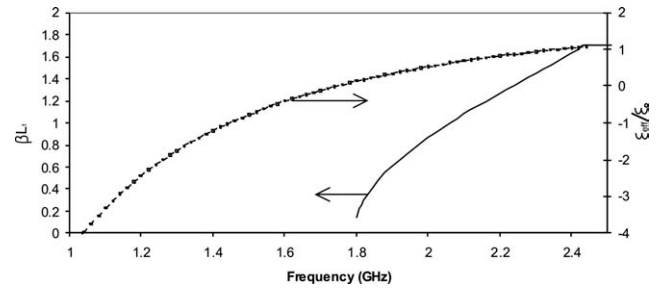
In Figure 2(a), the E-field distribution along the propagation direction x is depicted at the tunneling frequency (f_o). It is seen that the magnitude of the E-field is constant corresponding to $\beta = 0$. As a consequence a static-like behavior exists; hence, the tunneling frequency is completely independent of the tunnel length L_t, which can lead to miniaturized tunnels. In our case, we chose the length to be $L_t = 20$ mm, equivalent to 1/6 of the propagation wavelength ($\lambda/6$), compared with a $\lambda/2$ length of a conventional cavity.

For the dominant TE_{10} mode in rectangular waveguide, the symmetric plane along the transmission direction is equivalent to a magnetic wall. Therefore the tunnel can be cut into half without disturbing the field distribution [7]. The HM tunnel with the microstrip feed was fabricated with conventional printed circuit milling technology, and the walls of the tunnel were covered with thin copper layers. A schematic is shown in Figure 2(b).

Simulations of this tunnel are performed using [8]. Figure 3 shows the simulated and experimental transmission and reflection coefficients of the HM ENZ tunnel. Good agreement is seen between experiment and simulation. In the simulated case, the center frequency is 1.85 GHz, whereas in the experiment it is 1.8 GHz. An insertion loss of 1.1 dB for the experimental case is observed, whereas for the simulation it is 0.4 dB at the center frequency. The reflection loss is 19 dB for the experiment at the center frequency (f_o) and 30 dB in the simulation.
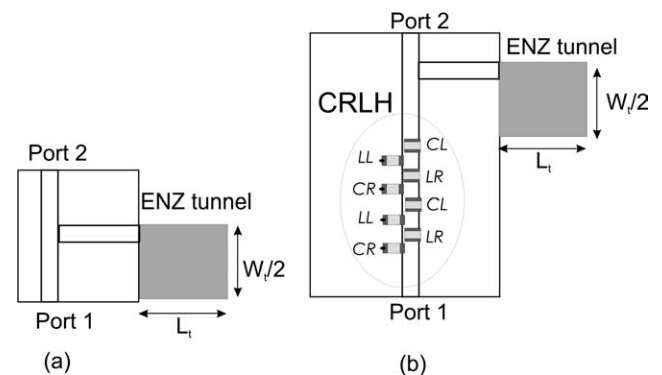
Furthermore by using Eq. (4), the phase constant is extracted from the simulated S parameters [9].

$$\beta \cdot L_t = \arccos\left(\frac{1 - S_{11}S_{22} + S_{21}S_{12}}{2S_{21}}\right). \quad (4)$$
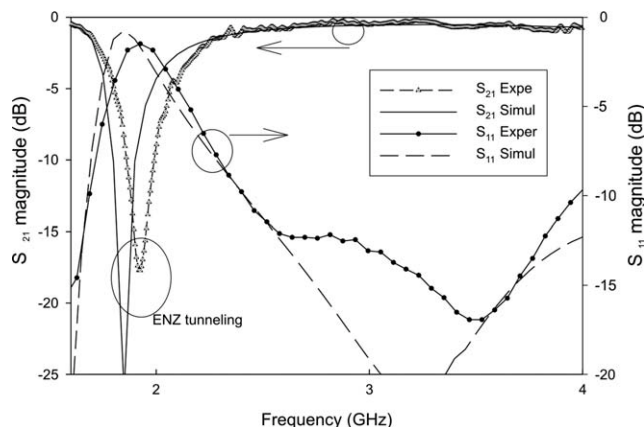
Figure 4 shows the dispersion diagram of βL_t from Eq. (4), along with the ε_{eff} parameter from Eq. (1). It is clear that at the center frequency the effective permittivity (ε_{eff}) is zero and the phase constant ($\beta = 0$), which satisfies the ENZ behavior.

3. NOTCH FILTER

To validate the concept of the ENZ tunneling as a notch filter, the tunnel described in the previous section was connected in a decoupling mode to a 50 Ω microstrip line as shown in Figure 5(a). One side of the tunnel is left open hence radiating into free-space at the tunneling frequency of 1.85 GHz. The structure is simulated using [8] and then implemented using conventional printed-circuit milling technology. The simulated and experimental responses are shown in Figure 6. As it can be seen from this figure, the decoupling frequency is centered at 1.85 GHz for the simulation and 1.92 GHz for the experiment. These discrepancies are thought to be because of manufacturing tolerances in the height and width of the tunnel, and substrate thickness tolerances. The insertion loss outside the tunneling frequency is about 1 dB for the simulation and 1.2 dB for the experiment,

Figure 4 Extracted effective permittivity (ε_{eff}), and phase constant β of ENZ tunnel

Figure 3 Simulated and experimental reflection and transmission coefficients of ENZ tunneling structure

Figure 5 (a) Decoupling ENZ tunnel, (b) Decoupling ENZ tunnel with CRLH wide band filter
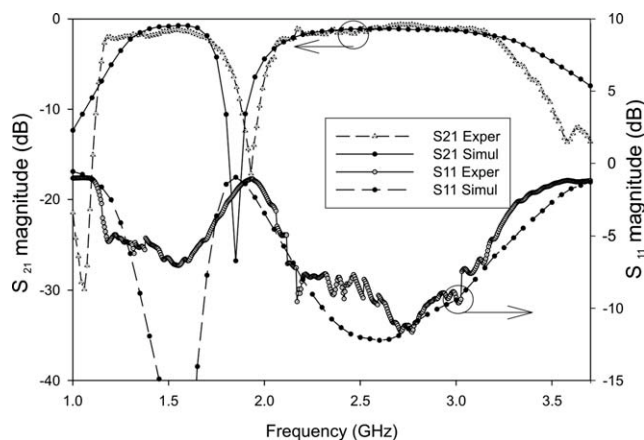
Figure 6 Simulated and experimental responses of decoupling ENZ tunnel

and the reflection losses are better than 12 dB throughout the pass band for both cases.

In addition, a two-cell CRLH filter is designed at a center frequency of 1.8 GHz and a fractional bandwidth of 110% following the procedure expanded in [10]. The design values of the CRLH unit cell are $C_R = 0.5$ pF, $L_R = 1.6$ nH, $C_L = 2.2$ pF, and $L_L = 4.3$ nH. This gives a -3 dB lower cutoff of $f_1 = 0.8$ GHz and an upper cutoff $f_2 = 2.8$ GHz. The circuit was implemented using standard surface mount devices (SMD).

To implement the notch filter, the ENZ tunnel is connected to the CRLH filter as shown in Figure 5(b). The CRLH filter along the tunnel structure is simulated using [8].

Figure 7 shows the simulated and experimental S_{21} and S_{11} responses. The simulated notch frequency is read at 1.85 GHz with a reflection loss of about 26 dB and an insertion loss of 1.3 dB. For the experimental response the return loss is 18 dB at the center frequency (1.94 GHz) and an insertion loss of 2 dB is recorded. The experimental 3 dB pass band is 2.14 GHz (from 1.15 to 3.29 GHz). There is a slight frequency shift of 0.2 GHz to lower frequencies in the experiment compared with the simulation. This frequency shift is thought to be because of parasitic effects of the SMD components, the effects of the vias to ground and the mismatch between the microstrip line width and the width of the SMD components. However, good agreement is observed between simulation and experiment.

Figure 7 Simulated and experimental S_{21} and S_{11} responses of notch filter composed by ENZ decoupling tunnel and CRLH band pass filter

4. CONCLUSIONS

A miniaturized HM substrate integrated ENZ tunnel has been demonstrated. It was shown that this structure allows only one frequency to tunnel through because of the static-like behavior when epsilon is near zero. Subsequently, the tunnel was connected to a CRLH filter in a decoupling mode to reject unwanted frequencies. Good agreement is seen between experimental and simulated results.

REFERENCES

1. M.G. Silveirinha and N. Engheta, Tunneling of electromagnetic energy through sub-wavelength channels and bends using epsilon-near-zero (ENZ) materials, Phys Rev Lett 97 (2006), 1–4.
2. W. Rotman, Plasma simulation by artificial dielectrics and parallel-plate media, IRE Trans Antennas Propag 10 (1962), 82–95
3. B. Edwards, A. Alù, M.E. Young, M.G. Silveirinha, and N. Engheta, Experimental verification of epsilon-near-zero metamaterial coupling and energy squeezing using a microwave waveguide, Phys Rev Lett 100 (2008), 1–4.
4. A. Alu and N. Engheta, Antenna matching in ε-near-zero metamaterial channels, IEEE International Workshop on Antenna Technology, iWAT 2009 (2009), 1–4.
5. B. Edwards, A. Alù, M.G. Silveirinha, and N. Engheta, Reflectionless sharp bends and corners in waveguides using epsilon-near-zero effects, J Appl Phys 105 (2009), 044905–044905.
6. A. Alu and N. Engheta, Dielectric sensing in ε-near-zero narrow waveguide channels, Phys Rev B: Condens Matter 78 (2008), 1–5.
7. W. Hong, B. Liu, Y. Wang, L. Qinghua, T. Hongjun, X.Y. Xiao, Y.D. Dong, Y. Zhang, and K. Wu, Half mode substrate integrated waveguide: A new guided wave structure for microwave and millimeter wave application, 14th International Conference on Infrared, Millimeter Waves and TeraHertz 2006, IRMMW-THz 2006, 219–219.
8. Ansoft HFSS software, version. 11.
9. G. Lubkowski, R. Schuhmann, and T. Weiland, Extraction of effective metamaterial parameters by parameter fitting of dispersive models, Microwave Opt Technol Lett 49 (2007), 285–288.
10. A. Lai, T. Itoh, and C. Caloz, Composite right/left-handed transmission line metamaterials, IEEE Microwave Mag 5 (2004), 34–50.

A DIELECTRIC CORRUGATED FEED HORN ANTENNA FOR SATELLITE COMMUNICATION APPLICATIONS

M. Secmen and A. Hizal
Electrical and Electronics Engineering Department, Middle East Technical University, Inonu Street, 06531, Ankara, Turkey; Corresponding author: msecmen@eee.metu.edu.tr

ABSTRACT: *In this study, a dielectric corrugated antenna, as being a feed horn antenna of the reflector antenna for satellite communication applications, is analyzed. The structure consists of a conical dielectric corrugated antenna terminated with a conductor hyperbolic (convex) plate. The antenna system provides a Gaussian beam within wide frequency bandwidth with its dielectric structure. The antenna is simulated and tested for its return loss and radiation performances, and the satisfactory results are obtained for C band satellite communication applications.* © 2010 Wiley Periodicals, Inc. Microwave Opt Technol Lett 52: 1709–1713, 2010; Published online in Wiley InterScience (www.interscience.wiley.com). DOI 10.1002/mop.25350